

PONTIFICIA UNIVERSIDAD CATÓLICA DEL PERÚ
FACULTAD DE CIENCIAS E INGENIERÍA



**Desarrollo de un detector juguete basado en el experimento CMS para la
búsqueda de partículas neutras con largo tiempo de vida**
**TRABAJO DE INVESTIGACIÓN PARA LA OBTENCIÓN DEL GRADO
DE BACHILLER EN CIENCIAS CON MENCIÓN EN FÍSICA**

AUTOR:

Lucía Ximena Coll Saravia

ASESOR:

Joel Jones Pérez

Lima, Agosto, 2020

Abstract

The Standard Model (SM) of particle physics consists in a description of all the known elementary particles and their interactions. As far as it is known, the SM has passed all experimental tests, but presents some imperfections such as the presence of neutrino masses and the hierarchy problem. This encourages to probe theories beyond the Standard Model (BSM) that could bring solutions to these problems. An interesting proposal is to search for neutral long lived particles (LLP). These type of particles have long decay lengths and can be generated by a variety of BSM models such as Supersymmetry (SUSY), which proposes a solution to the hierarchy problem, and the Seesaw Mechanism that generates massive neutrinos. The detection of the decay products of LLPs would contribute to the discovery of new physics. The objective of this work is to develop a toy detector based on C++ and Pythia8 with the purpose of creating a tool for searches of neutral long lived particles. All the features, including the geometric characteristics and the particle acceptance are constructed with information from the sub detectors of the CMS experiment. We use a Minimal SUSY process that violates R parity (RPVMSSM) to simulate processes producing LLPs in MadGraph5 and study the response of the toy detector. We conclude our simulation properly recreates important experimental conditions, and is suitable as a first step towards an international competitive particle physics tool.

A mi madre, ejemplo de esfuerzo, constancia y dedicación.

Sin ella nada es posible



Agradecimientos

Gracias a mi asesor, el Dr. Joel Jones, por las enseñanzas de todos estos años, desde que ingresé a la facultad. Agradezco la confianza y el apoyo constante durante estos últimos meses, han sido fundamentales para el desarrollo de esta tesis y, aún más importante, para mi crecimiento profesional.

Gracias al Grupo de Altas Energías PUCP por las tantas oportunidades de aprendizaje.

Gracias a Joaquin por toda la ayuda brindada, por escucharme en todo momento, sabiendo siempre qué decir y cómo hacerme reír. Por todo el apoyo de siempre.

Y gracias a mi familia, por creer en mi desde el primer día.

Contents

| | |
|--|-----------|
| List of Figures | v |
| List of Tables | v |
| 1 Introduction | 1 |
| 2 The CMS Experiment | 2 |
| 2.1 The Inner Detector | 4 |
| 2.2 The Electromagnetic Calorimeter | 5 |
| 2.3 The Hadronic Calorimeter | 6 |
| 2.4 The Muon System | 7 |
| 3 Long Lived Particles | 9 |
| 3.1 State of the art in searches for LLPs in CMS | 11 |
| 3.1.1 Experimental search for LLPs decaying into a pair of muons using only the CMS MS at $\sqrt{s} = 8$ TeV | 11 |
| 3.1.2 Experimental search for LLPs decaying into displaced dimuons using only the CMS MS at $\sqrt{s} = 13$ TeV | 13 |
| 3.1.3 Phenomenological study of LLPs with a prompt lepton trigger in the CMS MS | 14 |
| 3.1.4 Phenomenological study of heavy right handed neutrinos as candidates for LLPs decaying into leptons detected using the CMS MS | 17 |
| 3.1.5 Experimental search for LLPs at ATLAS MS | 19 |
| 4 Simulations | 22 |
| 4.1 The process | 22 |
| 4.2 The Toy Detector | 23 |
| 5 Summary and Conclusions | 31 |
| References | 31 |

List of Figures

| | | |
|----|--|----|
| 1 | CMS detector | 4 |
| 2 | ID and MS resolution | 5 |
| 3 | ECal resolution | 6 |
| 4 | HCal resolution | 7 |
| 5 | Drift tube chamber | 8 |
| 6 | Results from CMS experimental search | 13 |
| 7 | Results from search for LLPs decaying to two leptons | 15 |
| 8 | Results from phenomenological study of LLPs using a prompt lepton trigger | 17 |
| 9 | Results from phenomenological study of heavy neutrinos as LLPs decaying into leptons | 19 |
| 10 | Results from experimental search at ATLAS | 21 |
| 11 | Results from experimental search at ATLAS | 22 |
| 12 | Histogram of p_{Tnew} / p_T in the ID | 26 |
| 13 | Histogram of p_{Tnew} / p_T in the ECal. | 27 |
| 14 | Histogram of p_{Tnew} / p_T in the HCal. | 27 |
| 15 | Histogram of p_{Tnew} / p_T in the MS | 28 |
| 16 | Histogram of p_{Tnew} / p_T in all the sub detectors. | 28 |
| 17 | Histogram of ΔR_{min} | 30 |
| 18 | Histogram of ΔR_{max} | 30 |

List of Tables

| | | |
|---|---|----|
| 1 | Dimensions of sub detectors | 4 |
| 2 | Width and decay lengths of some non stable SM particles | 10 |
| 3 | Initial considerations for tag assignment | 24 |

1 Introduction

The SM provides a description of all the elementary particles and establishes the principles of their interactions. The model contains 12 fermions with spin $\frac{1}{2}$, four bosons with spin 1, and a fifth boson with spin 0. The fermions are divided in quarks and leptons. There are 6 quarks: up (u), charm (c), top (t), down (d), strange (s) and bottom (b), the first three with charge $\frac{2}{3}$, and the following with charge $-\frac{1}{3}$, all quarks carry colour charge; and 6 leptons: electron (e^-), muon (μ^-), tau (τ^-), electron neutrino (ν_e), muon neutrino (ν_μ) and tau neutrino (ν_τ), the first three with charge -1, and the following with no charge. The four spin 1 bosons are the force mediators, the photon (γ) mediates the electromagnetic interactions, the gluon (g) the strong interactions and the W^\pm and Z^0 bosons mediate the weak interactions. The spin 0 boson appears generates the mass of all the particles by the Brout-Englert-Higgs Mechanism, it is known as the Higgs boson. Quarks can interact via the three forces while charged fermions interact via the weak and electromagnetic force, and the neutrinos only with the weak force.

The SM has been almost entirely verified and found out to be experimentally successful. However, it is not complete. The SM presents several problems such as the predictions on neutrino masses: it defines neutrinos as massless, on the contrary, it has been proven that neutrinos have small masses by measuring neutrino oscillations. Moreover, it has a hierarchy problem related to the difference in magnitude between the small Higgs boson mass and the Planck scale.

Extensions to the SM trying to solve these problems are called beyond the SM (BSM) models. One solution to the neutrino mass problem is the Seesaw mechanism. This mechanism adds new heavy SM singlets coupling to the Higgs boson giving mass to the neutrinos through mixing. A possible solution to the hierarchy problem is the theory of Supersymmetry (SUSY), which assigns to every SM particle a SUSY partner with different spin.

The two possible solutions mentioned have regions of the parameter space where particles with long lifetimes can exist. These particles are called long lived particles (LLPs) and have not yet been thoroughly studied. In the present work, we are going to develop methods for studying these LLPs.

This document is going to be divided as follows: Section 1 is the introduction, in Section 2 we present all the relevant features of the CMS detector, in Section 3 we introduce the long lived particles and review some experimental searches and theoretical studies about them, in Section 4 we present the development of the toy detector and all its characteristics, finally, in Section 5 we summarize and conclude.

2 The CMS Experiment¹

The Large Hadron Collider (LHC) is a particle accelerator at CERN (European Organization for Nuclear Research). The principal objective is to discover and probe the mechanism for electroweak symmetry breaking, but it also studies theories Beyond the SM (BSM) such as super symmetry, dark matter, composite Higgs models, extra dimensions and new massive gauge bosons. It operates by accelerating two beams of protons and making them collide at extremely high energies. The very large circumference (about 27 kilometers) is important for generating a collision at the required energies. The LHC works with bunches of about 10^{11} protons. These bunches are at a distance of about 8 m (approximately a 25 ns flight) from each others, this means that the frequency of collision is 40 MHz ($\frac{1}{25}$ ns⁻¹). Considering that the inelastic proton-proton cross section is $\sigma_{pp} = 10$ mb and the transverse area of the beam line is $\sigma_{beam} = (10\mu\text{m})^2$, then the total rate of collision is given by

$$\text{Rate}_{\text{tot}} = \left(10^{11} \frac{\text{protons}}{\text{bunch}}\right)^2 \times \frac{10 \text{ mb}}{(10 \mu\text{m})^2} \times 40 \text{ MHz} = 4 \text{ GHz}$$

The most recent information from the LHC is collected from Run 2. The center of mass energy at this run is $\sqrt{s} = 13$ TeV and the integrated luminosity $L = 189.3 \text{ fb}^{-1}$.²

Other important parameters used in collider physics that are going to be mentioned along this work are:

¹All the information and figures in this section, unless specified, are extracted from [15].

²The barn (b) is the unit for scattering cross section. The luminosity is defined as the collision rate, and hence, the unit that is used to measure it is the b^{-1} .

- transverse momentum, which is the momentum in x and y (coordinates perpendicular to the beam line) as $\vec{p}_T = (p_x, p_y)$;
- pseudorapidity (η) that is defined as $\eta = \ln \left(\cot \left(\frac{\theta}{2} \right) \right)$ where θ is the angle generated by the vectors total momentum (\vec{p}) and the momentum in the beam line (p_z);
- ϕ is the azimuthal angle $\phi = \arctan \left(\frac{p_x}{p_y} \right)$;
- ΔR is the measurement of angular separation of two particles inside the collider and it is defined as $\Delta R = \sqrt{(\Delta\eta)^2 + (\Delta\phi)^2}$;
- finally, the momentum that is not detected ($\vec{p}_T^{miss} = -\sum p_T^{visible}$) is called missing transverse momentum. [22]

The amount of information generated by a collision of two proton beams is overwhelming and can not all be stored at once. There is a first step of hardware particle selection (trigger) where the particle must have certain characteristics for the event to be recorded, on the contrary, the information of the event is lost. This first hardware based trigger is called Level 1 (L1). Then, the data obtained passes through a second selection that is called High Level Trigger (HLT) customized by the user.

There are currently four experiments functioning in the LHC: A Toroidal LHC ApparatuS (ATLAS), Compact Muon Solenoid (CMS), A Large Ion Collider Experiment (Alice) and LHCb. This work is focused on the CMS experiment.[15]

CMS is designed to study fundamental particles and their interactions produced by a proton-proton collision. The detector (Figure 1) is mainly composed by four sub detectors: the Inner Detector (ID), the Electromagnetic Calorimeter (ECal), the Hadronic Calorimeter (HCal), and the Muon System (MS). It also includes a superconducting solenoid that generates a 4 T field. The dimensions of the sub detectors are given by Table 1, where R represents the radius of the cylinder and Z the half length.

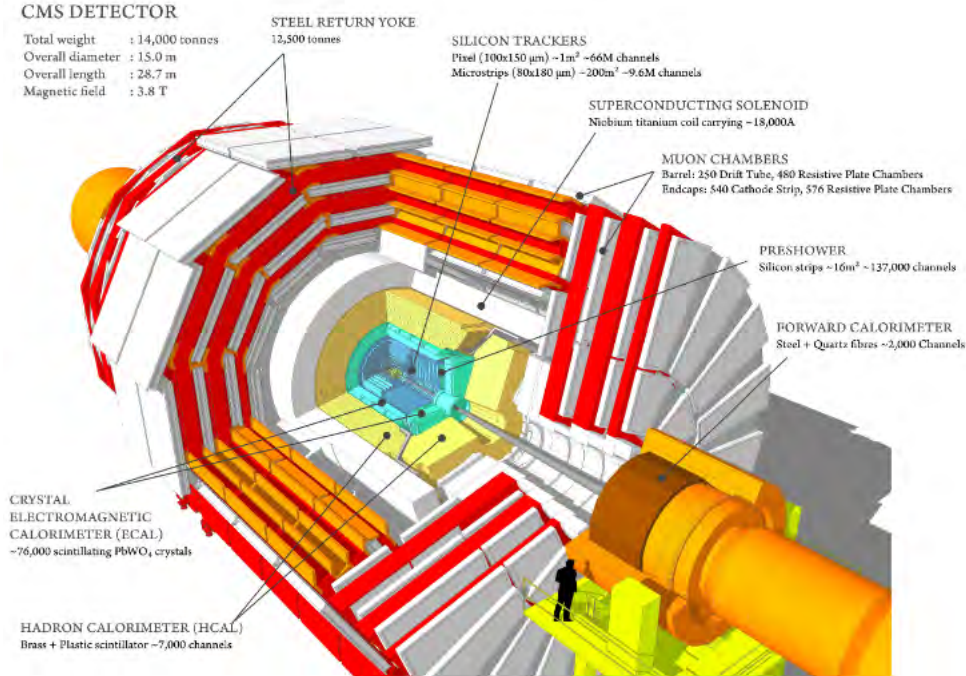


Figure 1: Image of the CMS detector taken from [12].

| Sub Detector | R_{min} [m] | R_{max} [m] | Z_{min} [m] | Z_{max} [m] |
|--------------|---------------|---------------|---------------|---------------|
| ID | - | 1.183 | - | 3.042 |
| ECal | 1.183 | 1.775 | 3.042 | 4.050 |
| HCal | 1.775 | 2.789 | 4.050 | 5.549 |
| MS | 4.169 | 7.409 | 6.6197 | 10.648 |

Table 1: Dimensions of the sub detectors obtained from [5]

2.1 The Inner Detector

The ID is designed to measure the trajectories of charged particles product of a proton-proton collision. The particles leave tracks in the ID, which can further be matched to a signal in another sub detector and give a finer precision in the measurement. At intervals of 25 ns, the ID receives the product of 2×10^{11} protons colliding, therefore it needs to have quick response and high granularity in order to manage the proper identification of the trajectories and assignment of them to the correct bunch.

The design is based on silicon detector technology and covers an area of diameter 2.5 m and

length 5.8 m around the nominal interaction point (IP)³. The pseudorapidity coverage is $|\eta| < 2.5$. As an example, in Figure 2 we show the transverse momentum resolution for muons, which we assume valid for all charged particles.

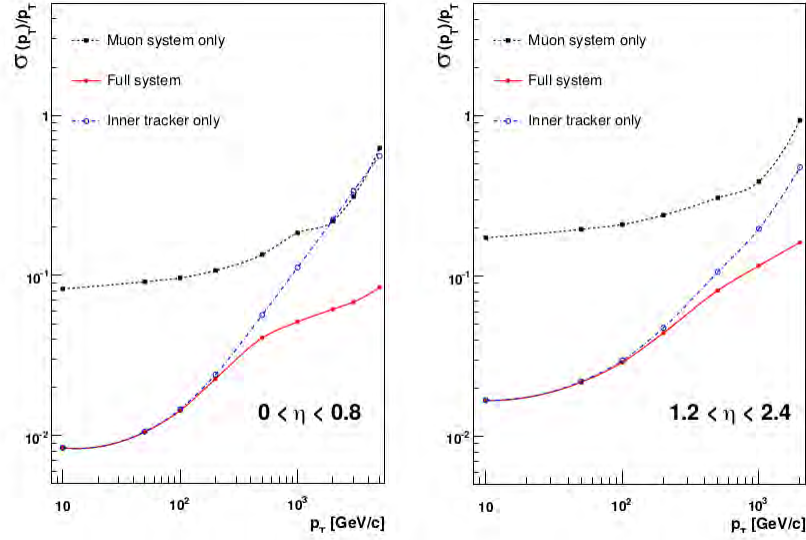


Figure 2: Muon transverse momentum resolution as function of transverse momentum. The blue dashed line is for the ID only, the black dashed line for the MS only, and the red line for the system ID + MS.

2.2 The Electromagnetic Calorimeter

The ECal generates a cascade of electromagnetic interactions whenever an electron or photon travels through it. The cascade consists of a shower of particles that release energy proportional to the energy of the incident particle, this way the ECal absorbs the particle and measures its energy. [18]

It is integrated by lead tungstate ($PbWO_4$) crystals. The barrel part covers $|\eta| < 1.479$ with 61200 crystals, and the two endcaps that cover $1.479 < |\eta| < 3$ with 7324 crystals each. The use of crystals make the ECal resistant to radiation product of the solenoid and have a fast response to signals.

³The IP is known as the position in the detector where the bunches collide. The nominal IP is the absolute center of the detector, this does not means that all interactions happen in this place, but on average

The energy resolution of the ECal (Figure 3) is parametrized by

$$\left(\frac{\sigma}{E}\right)^2 = \left(\frac{S}{\sqrt{E}}\right)^2 + \left(\frac{N}{E}\right)^2 + C^2$$

where S is the stochastic term, N the noise term which comes usually from the electronics, and C is a constant. This parameters were measured in 2004-2006 and are given by $S = 2.8\%$, $N = 0.12$ and $C = 0.3\%$.

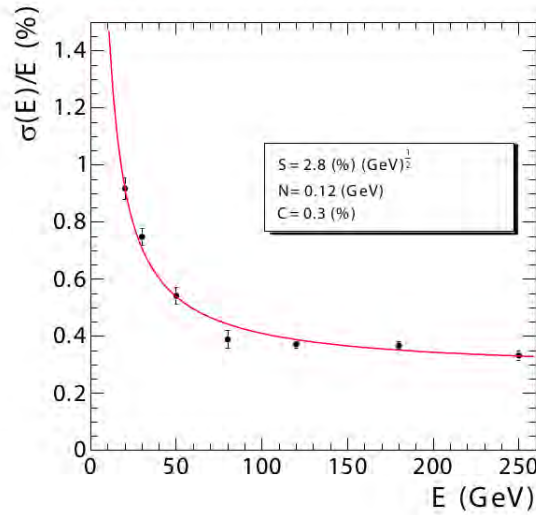


Figure 3: ECal percentage energy resolution function of energy.

2.3 The Hadronic Calorimeter

The HCal is in charge of absorbing and measuring the energy of all hadrons coming from the proton-proton collision. Similarly to the ECal, it has a barrel part that covers $|\eta| < 1.3$ and two endcaps that cover $1.3 < |\eta| < 3$. Both, the barrel and the endcaps, are compound by a scintillator of about 70 000 tiles, and an absorber that consists of 16 plates. An incident hadron interacts with the absorber producing a shower of less energetic particles, next, the scintillator produce a detectable signal.[18]

Although not shown in Figure 1, the HCal also consists on an outer hadron calorimeter placed outside the superconducting solenoid for identifying late starting showers. In addition, this sub

detector contains two forward calorimeters placed at 11.2 m from the IP for extending the pseudorapidity coverage up to $|\eta| = 5.2$. The jet transverse energy resolution for different ranges of η is shown in Figure 4.

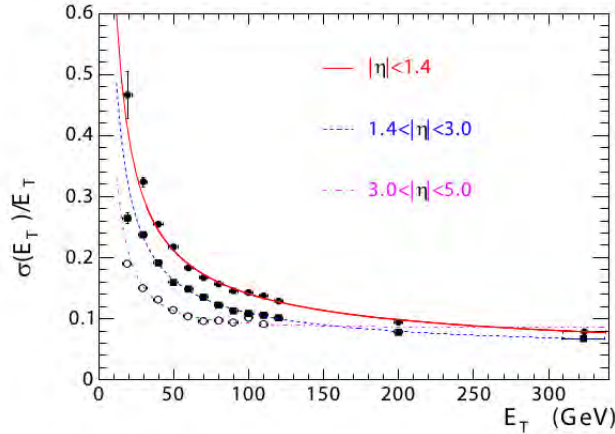


Figure 4: HCal jet transverse energy resolution function of energy for three different ranges of pseudorapidity.

2.4 The Muon System

The MS has three principal functions: identifying, reconstructing and triggering muons. It has 25 000 m² of detection plates along the three parts of the detector: the barrel and two endcaps.

The barrel has low muon background rate and uniform magnetic field produced by the superconducting solenoid. It is conformed by drift tubes (DT) chambers that cover a pseudorapidity of $|\eta| < 1.2$. The DT chambers are organized in four stations forming concentric cylinders around the beam line. The three inner cylinders contain 60 DT chambers each and the outer one 70. Figure 5 shows the composition and dimensions of a DT chamber. Each tube is filled with 85% Ar and 15% CO₂. When a muon passes through the tube it ionizes the gas and the generated electrons drift to the wire. The measurement of the drift time is an indirect measurement of the muon position. The arrangement of chambers is designed to obtain the best angle and time resolution, and to properly link muon hits from different station into one muon track.

The endcaps are integrated by cathode strips chambers (CSCs) which cover the range of $0.9 <$

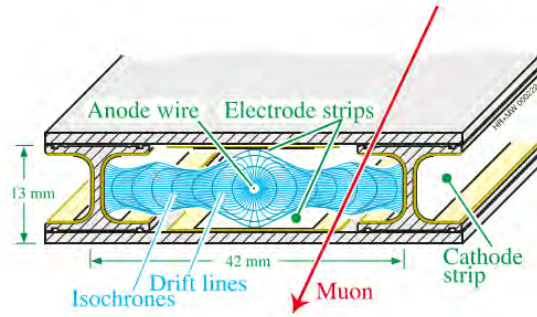


Figure 5: Drift Tube chamber composition and dimensions. [18]

$|\eta| < 2.4$. The CSCs have fast response time, fine segmentation and radiation resistance, which make them ideal for the high rates of background muons and non uniform magnetic field of this area. The chambers are located perpendicular to the beam line arranged as circular disks. There are 540 CSCs organized in four stations. The CSCs consist of six layers. each composed by 50% CO_2 , 40% Ar and 10% CF_4 . Between layers there is a plane of copper cathode strips and a plane of anode wires. A muon that passes through the gas ionizes it and generates electrons that drift to the wires. This induces a charge in the cathode strips leading to the measurement of the muon position. The CSCs are also able to reject non muon background signals and match hits with hits in other stations or in the ID.

Scattered among the DT chambers and the CSCs are 480 and 576 resistive plate chambers (RPCs), respectively. Each RPC is composed of two parallel plates separated a distance of 2 mm filled with 95.2% $\text{C}_2\text{H}_2\text{F}_4$, 3.5% C_4H_{10} and 0.3% SF_6 . A muon passing over these chambers ionizes the gas and generates an image charge that can be stored as signal. The time resolution of the RPC is about 2 ns, which is smaller than the time between bunch crossing at the LHC. For this reason the RPCs are able to identify muon tracks and designate it to the correct bunch crossing.

The reconstruction efficiency of simulated single muons is usually 95-99%. The offline momentum resolution for small η and p , and $p_T < 200$ GeV is around 9%. Around $p_T = 1$ TeV varies between 15% and 40% depending on η . The L1 trigger has a p_T resolution of 15% in the barrel and 25% in the endcaps. The exact function is given in Figure 2.

3 Long Lived Particles

As is well known, the SM is not complete. There are a group of theories that aim to give solutions to the imperfections of the SM. New particles can be postulated that interact with the SM and whose lifetimes are longer than those of non-stable SM particles. The latter particles decay as described in the Table 2. Long Lived Particles (LLPs) are particles produced in the proton-proton collision and are able to propagate a macroscopic distance before decaying. If the LLP is neutral, it produces a Displaced Vertex (DV). If it does not decay inside the detector, then has to be considered as missing energy.

The probability for decay of a particle is

$$P_{dec}(t_1, t_2) = \int_{t_1}^{t_2} dt \frac{1}{\tau_{lab}} \exp\left(-\frac{t}{\tau_{lab}}\right)$$

where τ_{lab} is the lifetime of the particle in the laboratory reference frame. By changing the integration variable from time t to distance x we are able to calculate the probability of a particle decaying inside the detector. It is given by:

$$P_{dec}(x_1, x_2) = \int_{x_1}^{x_2} dx \frac{m}{|\vec{p}|\tau_{rest}} \exp\left(-\frac{x m}{|\vec{p}|\tau_{rest}}\right)$$

where τ_{rest} is the lifetime of the particle at rest, m the mass and $|\vec{p}|$ the absolute value of the momentum of the particle. All the mentioned variables must be in the same measurement system, SI units or natural units. Integrating this equation we find that the probability of a particle decaying inside the detector at $\eta = 0$ is

$$P_{in} = 1 - \exp\left(-\frac{R_{max} m}{|\vec{p}|\tau_{rest}}\right)$$

where $R_{max} = 7.409$ meters is the maximum radius of the detector (Table 1). We also are able to compute the probability of the particle decaying inside one specific sub detector, as an example,

we show the results for the MS:

$$P_{MS} = \exp\left(-\frac{R_{min} m}{|\vec{p}|\tau_{rest}}\right) \left[1 - \exp\left(-\frac{\Delta R m}{|\vec{p}|\tau_{rest}}\right)\right]$$

where $R_{min} = 4.169$ meters is the minimum radius of the MS and $\Delta R = 3.240$ meters its width.

In Table 2 we present the decay width of some non stable SM particles obtained from [24]. The decay length ($c\tau$) is calculated using the relation:

$$L = \frac{c\hbar}{\Gamma}$$

where L is the distance travelled by the particle and Γ is the decay width at rest. The constants c and \hbar are the speed of light and the Planck's constant, respectively, and τ is the mean lifetime of each particle.

| | Particles | Γ [GeV] | $c\tau$ [mm] |
|---------|---------------------|------------------------------|-------------------------------------|
| Bosons | W | 2.085(42) | $(9.471 \pm 0.191) \times 10^{-14}$ |
| | Z | 2.4952(23) | $7.9136(71) \times 10^{-14}$ |
| | H _{theory} | $4.07(16) \times 10^{-3}$ | $4.85(19) \times 10^{-11}$ |
| | H _{exp.} | <0.013 | $>1.518 \times 10^{-11}$ |
| Leptons | μ | $29.9800(3) \times 10^{-20}$ | $658.6384(7) \times 10^3$ |
| | τ | $2.268(4) \times 10^{-12}$ | $8.703(15) \times 10^{-2}$ |
| Quarks | t | 1.42(19) | $1.39(19) \times 10^{-13}$ |
| Mesons | π^\pm | $2.5301(5) \times 10^{-17}$ | $7.8045(15) \times 10^3$ |
| | π^0 | $7.74(16) \times 10^{-9}$ | $2.55(5) \times 10^{-5}$ |
| | K_S^0 | $7.356(3) \times 10^{-15}$ | $2.684(1) \times 10^1$ |
| | K_L^0 | $1.287(5) \times 10^{-17}$ | $1.534(6) \times 10^4$ |
| | D^\pm | $6.333(43) \times 10^{-13}$ | $3.118(21) \times 10^{-1}$ |
| | D^0 | $1.607(6) \times 10^{-12}$ | $1.229(4) \times 10^{-1}$ |
| | D_S^\pm | $1.306(10) \times 10^{-12}$ | $1.512(11) \times 10^{-1}$ |
| | J/ψ | $9.29(28) \times 10^{-5}$ | $2.130(6) \times 10^{-9}$ |
| | B^\pm | $4.021(10) \times 10^{-13}$ | $4.911(12) \times 10^{-1}$ |
| | B^0 | $4.336(11) \times 10^{-13}$ | $4.554(12) \times 10^{-1}$ |

Table 2: Width and decay lengths of some non stable SM particles. The values are taken from [24] with the exception of the Higgs theoretical value that was taken from [19].

3.1 State of the art in searches for LLPs in CMS

In this sub section we are going to review some publications that include theoretical studies and experimental searches for LLPs that are focused on detecting them mainly with the MS, and are of principal interest to this work.

This searches can be complemented with a search of LLPs decaying leptons only using the ID [21] and with a search for LLPs that decay into dijets creating a vertex in the ID [13]. Some similar studies made in different experiments should be mentioned, as a search for neutral LLPs decaying into lepton jets in the ATLAS experiment at $\sqrt{s} = 8$ TeV [3] and a search for LLPs decaying into two muons in the Fermilab Tevatron at $\sqrt{s} = 1.96$ TeV [4].

3.1.1 Experimental search for LLPs decaying into a pair of muons using only the CMS MS at $\sqrt{s} = 8$ TeV

CMS Collaboration published in 2015 a search for LLPs decaying into two muons and reconstructing them only using the muon chambers [14]. This was accomplished using data from Run 1 of the LHC, the center of mass energy was $\sqrt{s} = 8$ TeV and the luminosity $L = 20.5 \text{ fb}^{-1}$.

The work was done employing two benchmark models. The first one proposes the LLPs as spinless bosons (X) pair produced from the decay of a non-SM Higgs ($H^0 \rightarrow XX$), which is produced by gluon gluon fusion. The X boson decays into two muons ($X \rightarrow \mu^+ \mu^-$) with a decay length chosen to be 20, 200 and 2000 cm. In the second model, a pair of scalar quarks (squarks \tilde{q}) is considered, each of them decay into a quark and a neutral fermion (neutralino $\tilde{\chi}$), the latter being the candidate for LLP, ($\tilde{q} \rightarrow q\tilde{\chi}$). The neutralino decays into two muons and a neutrino ($\tilde{\chi} \rightarrow \mu^+ \mu^- \nu$) with approximately 200 cm of mean transverse decay length given by the chosen coupling⁴.

The events are selected by a trigger requiring two muons in the MS with $p_T > 23$ GeV. For avoiding cosmic muons that usually appear as back to back muons on the detector, the angle between them must not be greater than 2.5 rad. The trigger also requires that the distance between the

⁴In SUSY models, this coupling violates R-parity.

primary vertex (PV) and the nominal IP be less than 2 cm. The PV is the reconstructed position of the particles collision.

Over the reconstructed muon candidates a last adjustment for minimizing possible biases is applied, this generates refitted stand alone (RSA) muons. The RSA muons are required to have $p_T > 26$ GeV and $|\eta| < 2$. If those which fulfill this restriction can be matched to a track in the ID with $p_T > 10$ GeV, they are rejected as a displaced particle, and thus eliminated from the analysis. It is considered a match if ΔR between the two tracks is less than 0.1. It is also required that $|d_0|/\sigma_d > 4$ for every displaced muon, where $|d_0| = |xp_y - yp_x|/p_T$ is the transverse impact parameter and σ_d its resolution.

The process of choosing the LLPs candidates begins with pairing all possible combinations of selected muons, each pair of muons is called a dimuon, with the two muon tracks forming a displaced vertex (DV). The invariant mass of a dimuon must be at least 15 GeV. If there is a muon assigned to more than one DV that pass all the requirements below, the chosen dimuon is the one that has a better fit with respect to the hits in the sub detectors. Since the trigger loses efficiency if the two muons are too close to each other, it is required that the dimuon satisfy $\Delta R > 0.2$. The last requirement is for the LLPs to have transverse decay length significance $L_{xy}/\sigma_{xy} > 12$, where L_{xy} is the transverse distance the LLP propagates from the PV to the DV and σ_{xy} its resolution (approximately 3 cm). Given the dimensions of the MS, L_{xy} must be less than 500 cm for the muons to be detected.

In Figure 6 the results of this search are shown for the spinless boson (X) model. The 95% confident level (CL) upper limits of $\sigma(H^0 \rightarrow X X)B(X \rightarrow \mu^+\mu^-)$ are presented for Higgs masses equal to 125, 200, 400 and 1000 GeV; $\sigma(H^0 \rightarrow X X)$ refers to the cross section of the SM like Higgs decaying to two X bosons and $B(X \rightarrow \mu^+\mu^-)$ refers to the branching ratio of the boson X decaying into two muons. After all the event selection, no events were observed.

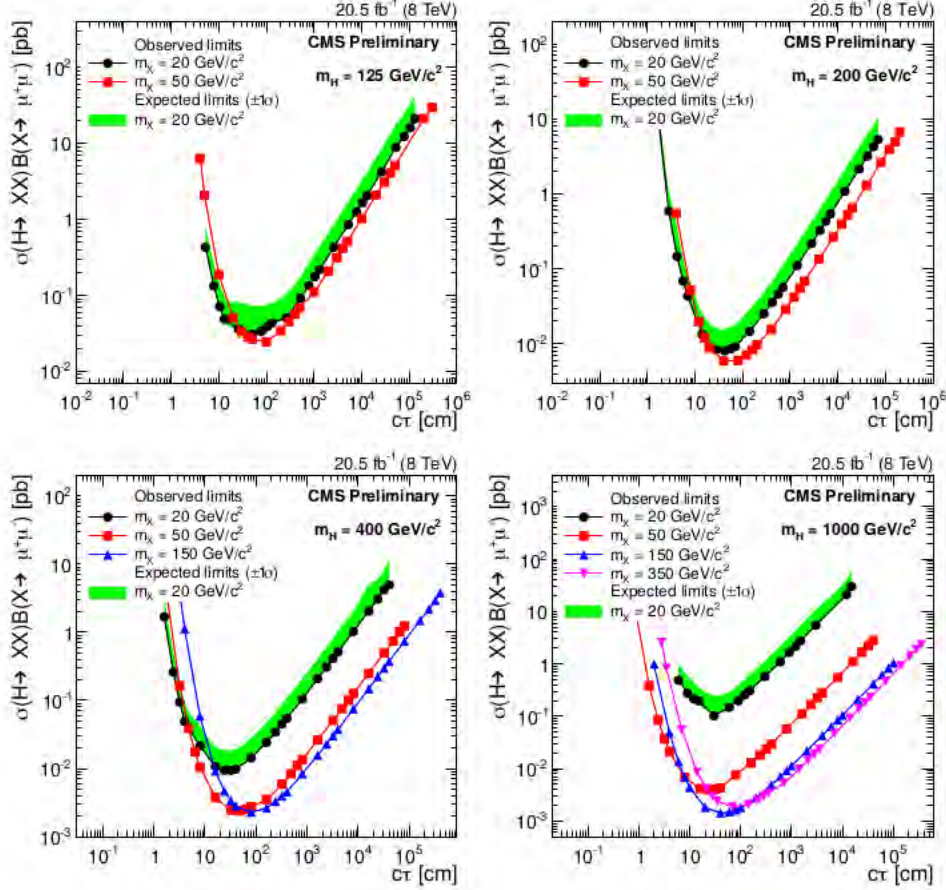


Figure 6: It is shown the upper limits of $\sigma(H^0 \rightarrow X X)B(X \rightarrow \mu^+\mu^-)$ at 95% CL for different Higgs masses. The green shaded region represents the $\pm 1\sigma$ variations of the 20 GeV X boson mass. [14]

3.1.2 Experimental search for LLPs decaying into displaced dimuons using only the CMS MS at $\sqrt{s} = 13$ TeV

This search [18] looks for two muons product of a long lived scalar boson X coming from the decay of a BSM Higgs ($H \rightarrow X X$), reconstructed using only the MS with center of mass energy $\sqrt{s} = 13$ TeV and luminosity $L = 36.3\text{fb}^{-1}$. This search is based on [14, 21, 1] and represents an improvement of [14] over the selection and reconstruction of signal, and also the estimation of background. For this search is required the new bosons to decay between the IP and the beginning of the MS. The lifetimes used for them are chosen to be 3, 30, and 250 cm.

The detector L1 trigger cuts for the generated muons are $p_T > 25$ GeV, $|\eta| < 2$ and $L_{xy} < 500$ cm. After this, restrictions from the High Level Trigger (HLT) are applied. For transverse

momentum, $p_T > 28$ GeV to reduce possible QCD background, the angle between all the possible pairs of detected muons must not be greater than 2.5 rad ($\cos \theta_{\mu\mu} > -0.8$), and the invariant mass of the system must be greater than 10 GeV.

The search uses primarily displaced standalone (DSA) muons which are defined from the following cuts: they must be reconstructed using at least two muon stations, their p_T must be greater than 10 GeV and the relative p_T uncertainty must be less than 100%. They compared DSA to RSA muons described in [14] (see Section 3.1.1) and opt for DSA muons, the reason was their improved p_T resolution and higher reconstruction efficiency. All the muons that pass the HLT and are DSA muons are considered for the analysis.

This search defines dimuons differently from those in Section 3.1.1. The four muons with greatest p_T are chosen, and grouped into pairs of opposite charge ideally coming from the same DV. A dimuon is defined by a pair of DSA muons satisfying: $\Delta R < 0.4$, $\chi_{vertex}^2 < 20$, $L_{xy}/\sigma_{xy} > 6$ and $|\Delta\phi| < \pi/4$. The search considers at most two dimuons, assuming that the LLPs are produced in pairs. Considering that the maximum numbers of dimuons formed is $n(n-1)/2$, where n is the number of muons, then, if there are zero or one muon, no dimuon is detected and it can be concluded that both LLPs decayed outside the detector. If there are two muons, up to three dimuons can be constructed, and the one with the better fit of the common vertex is chosen, this is interpreted as one LLP decaying inside the detector. For more muons, two dimuons are chosen from the better fit of the common vertex, then the two LLPs decays are detected inside the detector.

Figure 7 shows the upper limits of $\sigma(H^0 \rightarrow X X)B(X \rightarrow \mu^+\mu^-)$ with 95% CL for the Higgs mass equal to 1000 GeV and the different masses of the X boson (350, 150, 50 and 20 GeV). After applying all the cuts mentioned before, there was no excess over the SM expected background.

3.1.3 Phenomenological study of LLPs with a prompt lepton trigger in the CMS MS

The phenomenological study [9] seeks to demonstrate the potential that the CMS MS has for DV searches by analyzing results of a variety of searches with different applied cuts. We will focus on their analysis of heavy neutral leptons (HNLs). The model of HNLs introduces a Majorana fermion

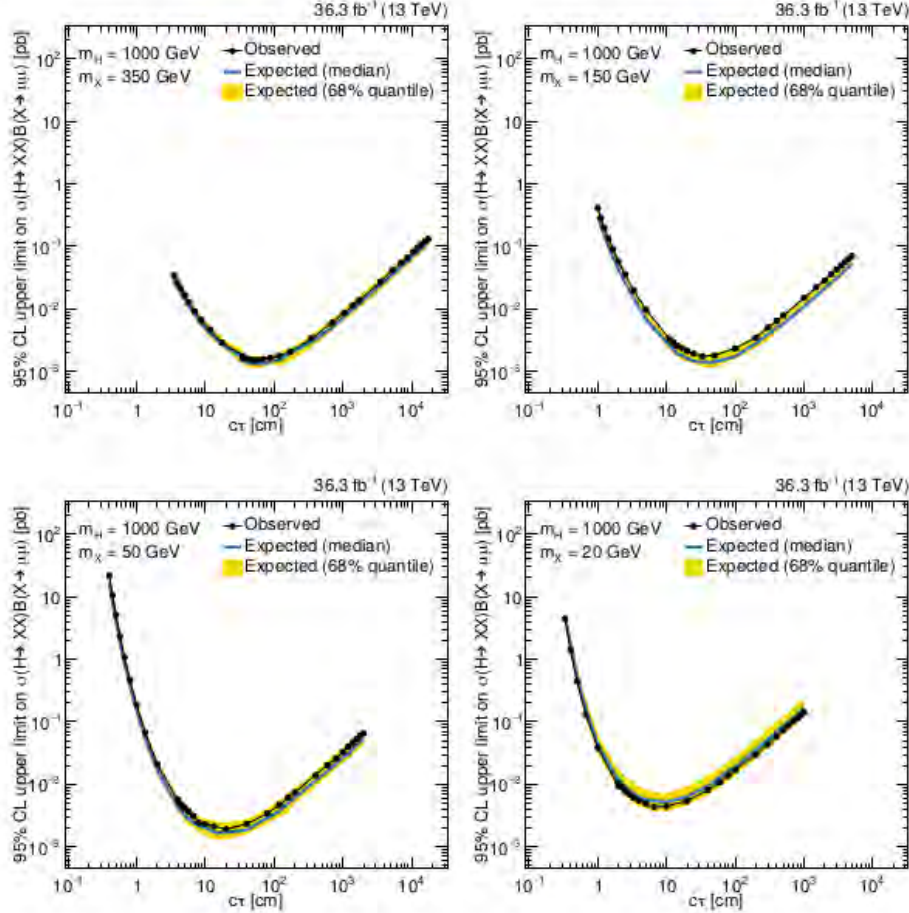


Figure 7: The upper limits of $\sigma(H^0 \rightarrow X X)B(X \rightarrow \mu^+\mu^-)$ with 95% CL are shown for $m_H = 1000$ GeV and different m_X . The black dots are the observed limits, the blue line the expected median and the yellow shaded region the central 68% quantile. [18]

singlet (N) coupled to the the SM $SU(2)_L$ lepton and the Higgs doublet. This coupling introduces mass to the HNL and generates an interaction with the SM left handed neutrino ν_ℓ .

An event must have a prompt lepton for satisfying the requirements of the single lepton trigger. If it is a muon, it must have with $|\eta| < 2.4$ and $p_T > 25$ GeV and if it is an electron $|\eta| < 2.5$ and $p_T > 30$ GeV.

They work with “long DVs”, which are events that, in addition to the prompt leptons already mentioned, must have two displaced muons with $|\eta| > 2.4$ and $p_T > 5$ GeV from which a DV can be reconstructed. This DV must satisfy the following cuts: the vertex must be displaced at least 2 cm from the PV and a maximum 300 cm (700 cm) in the transverse plane (beam line).

They define the number of decay events that should be detected as

$$N_{Events} = N_{Parents} \times Br_{prod} \times P_{decay} \times \epsilon$$

where $N_{Parents}$ is the number of particles that produce the LLPs, Br_{prod} is the branching ratio for decays of the parent into final states involving the LLP, ϵ is the fraction of decays of the LLPs that happen inside the detector volume and pass the selection criteria, it is proportional to the efficiency of selection and reconstruction, and to the branching ratio of decay of LLPs. the quantity P_{decay} is the decay probability defined as

$$P_{decay} = \int d\theta dp f(p, \theta) \times \left(\exp \left[-\frac{l_{min}}{c\tau\gamma} \right] - \exp \left[-\frac{l_{max}}{c\tau\gamma} \right] \right)$$

where l_{min} and l_{max} are the minimum and maximum lengths where the LLP decay can be detected, τ is the proper lifetime of the LLP, γ is the Lorentz factor and the function f is the distribution of the LLPs that passed the selection criteria. Notice that this formula assumes the particle is at speed of light.

The principal production process of HNLs with mass greater than 5 GeV is the decay of the W bosons with a total production cross section determined to be $\sigma_W = 190$ nb. They use the HeavyN model of MadGraph5 [7] for the simulations. The selection efficiencies were computed and lead to the conclusion that they are independent of the mass of the HNLs in the range of 1 - 20 GeV.

Results are shown in Figure 8. Each graph corresponds to the mixing with a different lepton flavor. The blue short dashed line is the area excluded by the selection criteria they applied called "realistic", the blue long dashed line excludes the area by the selection criteria applied in [20] called "optimistic", both denoted DV_L (long DV). The green line is for DV_S , that stands for short DV, which vertices displaced shortly, about 0.3 m. The exclusion of this area was defined on studies with the ID of ATLAS [17, 16]. The black dashed line illustrate the HNLs parameters leading to $l_{decay} = 300$ cm.

They finally conclude that it is possible to explore the parameter space with masses smaller than

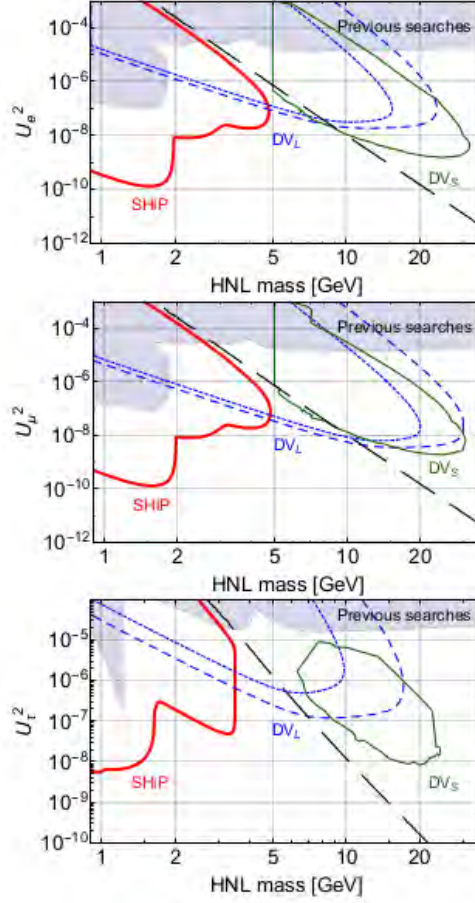


Figure 8: Limits on HNL mass mixing. Each plot shows bounds for a different lepton flavour: at the top U_e^2 , middle U_μ^2 and bottom U_τ^2 . [9]

20 GeV and mixing up to $U^2 \sim 10^{-18}$, using the long DVs. This study is particularly interesting since it triggers a prompt lepton which has not been done in any of the other studies cited in this work.

3.1.4 Phenomenological study of heavy right handed neutrinos as candidates for LLPs decaying into leptons detected using the CMS MS

A phenomenological study of a minimal renormalizable Abelian extension for the SM characterized by an extra $U(1)'$ symmetry that has a new scalar field heavier than the SM-like Higgs is presented in [5]. It predicts the existence of a heavy right handed neutrino (N) per lepton flavor that couples to the new scalar and can be proposed as LLP.

In this model, the production of a pair of heavy neutrinos (HN) coming from the SM-like Higgs (H^0) cross section is given by

$$\sigma(pp \rightarrow H^0 \rightarrow NN) = \cos^2 \alpha \sigma(pp \rightarrow H^0)_{SM} \frac{\Gamma(H^0 \rightarrow NN)}{\cos^2 \alpha \Gamma_{SM}^{tot} + \Gamma(H^0 \rightarrow NN)}$$

where $\sigma(pp \rightarrow H^0)_{SM}$ and Γ_{SM}^{tot} are the SM Higgs production cross section and total decay width, respectively. $\Gamma(H^0 \rightarrow NN)$ is the partial decay width of the SM-like Higgs into two HNs and has the form

$$\Gamma(H^0 \rightarrow NN) = \frac{3}{2} \frac{m_N^2}{x^2} \sin^2 \alpha \frac{m_{H^0}}{8\pi} \left(1 - \frac{m_N^2}{m_{H^0}^2}\right)^{\frac{3}{2}}$$

where x is the vacuum expectation value (VEV) of the new scalar. The parameter alpha is the mixing angle in the scalar sector, it defines how the width and cross section are going to scale with respect to the SM. If $\alpha = 0$ then $\Gamma(H^0 \rightarrow NN)$ is zero and the cross section of the SM is recovered.

The data used comes from the LHC Run 2 with $\sqrt{13}$ TeV. For the analysis, they separate the detector into two regions where the LLPs can decay. Region 1 is between the end of the ID, where a track can not be reconstructed, and before the MS, to have the possibility to observe hits in there. This area of the detector is a cylinder of radius R and half length z , with $0.5 \text{ m} < R < 5 \text{ m}$, $|z| < 8$. Region 2 selects events that decay only in the ID, the cylinder of detection is $0.1 \text{ m} < R < 0.5 \text{ m}$ and $|z| < 1.4$. We are going to focus on region 1. In this area they impose the restriction $L_{xy}/\sigma_{xy} > 12$, where L_{xy} is the transverse decay length and σ_{xy} its resolution (approximately 3 cm).

The HN decay into charged leptons that can be electrons or muons. The decay chains are:

$$\begin{aligned} N_R &\rightarrow l^\pm W^\mp &&\rightarrow l^\pm l'^\mp \nu_{l'} \\ &&&\rightarrow l^\pm q \bar{q} \\ N_R &\rightarrow \nu_l Z &&\rightarrow \nu_l l'^+ l'^- \\ &&&\rightarrow \nu_l q \bar{q} \\ &&&\rightarrow \nu_l \nu_{l'} \bar{\nu}_{l'} \end{aligned}$$

In an event there must be four leptons, two leading (the most energetic ones) and two sub leading. A pair leading - sub leading lepton establishes a DV. The leading leptons must have a $p_T > 26$ GeV, $\eta < 2$ and $\Delta R > 0.2$, the sub leading leptons $p_T > 5$ GeV. For avoiding cosmic muons an extra constraint is added to the cosine between two muons, $\cos \theta_{\mu\mu} > -0.75$.

The cross section of the production of heavy neutrinos is presented in Figure 9, as function of the mass of a heavy Higgs (H2). H2 couples to the SM-like Higgs of mass 125.09 GeV. They identified between two to four muons in the MS. After applying all the cuts, the total expected number of events (the sum of expected number of events for two, three and four muons) was 33 at a luminosity of $L = 100 \text{ fb}^{-1}$. This considering the mass of N equal to 40 GeV, the mass of the light neutrinos as 0.75 GeV, the decay length equal to 1.5 m, and the cross section $\sigma(pp \rightarrow H^0 \rightarrow NN) = 332.3 \text{ fb}$.

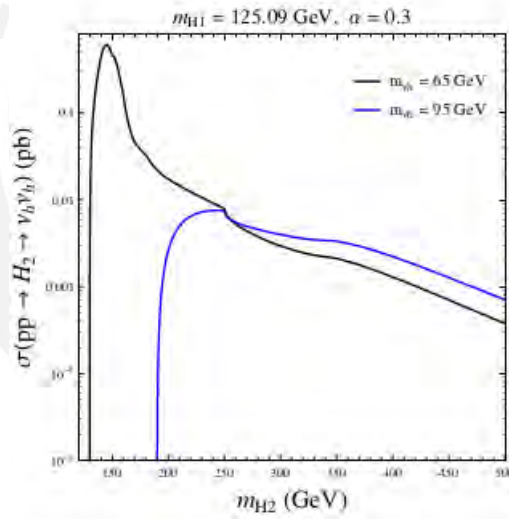


Figure 9: The cross section of pair production of heavy neutrinos is presented, as function of the mass of H2. The parameter alpha is 0.3. The black line corresponds to a heavy neutrino mass of 65 GeV and the blue one to a mass of 95 GeV. [5]

3.1.5 Experimental search for LLPs at ATLAS MS

As a reference, a study by ATLAS Collaboration [2] is considered. They search for LLPs in the ATLAS muon spectrometer with center of mass energy $\sqrt{s} = 13 \text{ TeV}$. Three benchmark models

are taken into account: Scalar portal, Higgs portal baryogenesis, Stealthy SUSY. The scalar portal model proposes a SM-like Higgs (ϕ) produced in the p-p collision, decaying into two long lived scalars (s), each of them decaying into two fermions. The Higgs portal baryogenesis model, again, proposes a SM-like Higgs boson (h) produced promptly that decays into two long lived Majorana fermions (χ), each of them decay into three fermions. Finally, the Stealthy SUSY model introduces a long lived singlino (\tilde{S}), produced from a prompt gluino (\tilde{g}) with a prompt gluon jet. The \tilde{S} decays into two gluons and a gravitino (\tilde{G}). The analysis consists on three strategies: searching for two MS vertex (2MSVx), and searching for one MSVx and accompanying objects that can be missing transverse momentum ($p_T^{\vec{miss}}$) or prompt jets.

All the candidates for LLPs are selected by the Muon RoI trigger which is a signature driven trigger for the MS of ATLAS detector that selects isolated signal-like events and non isolated background-like events. The muon trigger system covers $|\eta| < 2.4$ and the muon chambers system $|\eta| < 2.7$. For p_T lower than 10 GeV an event is required to have hits in at least three layers of the four layers in the barrel, or in the two outer layers of the endcaps, this defines a region of interest (RoI). For higher p_T , it is required additional hits in the external layer of the barrel are required. The trigger requires a cluster of three muon RoIs in the barrel or four in the endcaps. This trigger is efficient for hadronic decays of LLPs that occur between the outer region of the HCal and the first half of the MS.

Jets detected on the calorimeter with transverse energy threshold greater than 10 GeV and $|\eta| < 4.9$ are reconstructed using the anti- k_t algorithm with FastJet 2.4.3 package[11]. For computing the $p_T^{\vec{miss}}$ the search considers electrons with $p_T > 10$ GeV and $|\eta| < 2.47$, and for muons with $p_T > 10$ GeV and $|\eta| < 2.7$.

For an event to be selected, it must meet the following criteria: satisfy the Muon RoI cluster trigger, have a primary vertex with two or more tracks in the ID with $p_T > 400$ MeV, have at least one MS displaced vertex, and events in the MS barrel ($|\eta| < 0.7$) or endcaps ($1.3 < |\eta| < 2.5$) must have more than 250 hits.

The 2MSVx strategy works principally when the LLP is pair produced and decays into hadrons

between the last layer of the HCal and the first half of the MS. In this instance the transverse energy must be greater than 5 GeV for high p_T tracks, it is also required $\Delta R < 0.3$ in the barrel and $\Delta R < 0.6$ in the endcaps. For low p_T tracks $\sum p_T < 10$ GeV and $\Delta R < 0.2$ in the barrel and endcaps. Notice there is no overlap between the high and low p_T tracks, since we have four muons, two per MS vertex, for high p_T tracks the sum of p_T should be at least 20 GeV.

For the $1MSVx + p_T^{miss}$ strategy, all jets with transverse energy greater than 15 GeV are considered and p_T^{miss} must be greater than 30 GeV. The minimum separation from the analyzed MS vertex to an object is given by $\Delta R_{min} = \min(\Delta R(vertex, closest\ jet), \Delta R(vertex, closest\ track))$ which is demanded to be greater than 0.8. The angle between the p_T^{miss} vector and the direction of the DV $|\Delta\phi(p_T^{miss}, MSVx)|$ must be less than 1.2. For events in the barrel the search requires more than 1200 hits and in the endcaps 1500 hits.

For the $1MSVx + jets$ strategy, the following cuts are imposed: detect in the barrel 2000 hits, ΔR_{min} should be greater than 0.3, and there must be two jets with transverse energy greater than 150 GeV and $\Delta R(jet, vertex) > 0.7$. In the endcaps there must be at least 2500 hits, $\Delta R_{min} > 0.4$ and two jets with transverse energy greater than 250 GeV and $\Delta R(jet, vertex) > 0.7$.

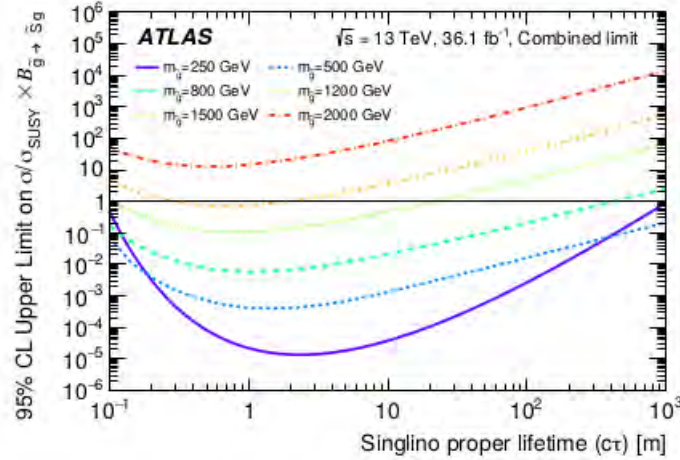


Figure 10: The upper limits at 95% CL of $\sigma/\sigma_{SUSY} \times B(\tilde{g} \rightarrow \tilde{S}g)$ are graphed with respect to the proper lifetime of the singlino for different gluino masses. [2]

The observed limits are shown in Figure 10 for the Stealthy SUSY model and Figure 11 for the scalar portal model. In both cases the limits were obtained from the three strategies employed and

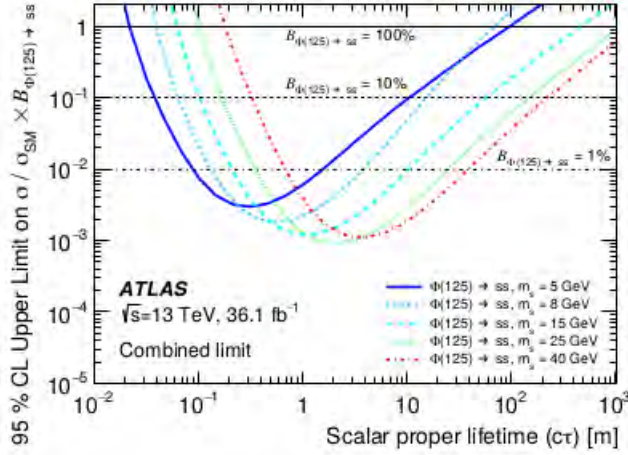


Figure 11: The upper limits at 95% CL of $\sigma/\sigma_{SM} \times B(\phi \rightarrow s s)$ are graphed with respect to the proper lifetime of the scalar for different masses. The mass of the Higgs boson is 125 GeV. [2]

have 95% CL. In the SUSY model graph, each line represents a given mass to the gluino and, in the scalar portal model graph, each line represents a given mass of the s boson coming from a 125 GeV Higgs boson. After all the analysis, no significant excess is found.

4 Simulations

4.1 The process

In this work we used MadGraph5_aM@ (MG5) to simulate an R parity violation (RPVMSSM) process. MadGraph5 [7] is an environment based on C++ for simulating parton showers and calculating cross sections of SM and BSM processes. We simulated this process using a simplified model of LLPs from the repository in [6]. In this case we simulated a pair production of sneutrinos ($\tilde{\nu}_e$) that decay as:

$$\tilde{\nu}_e \rightarrow e^- \mu^+.$$

When running MG5 with the specified process, a Les Houches event (LHE) File [8] is generated. It contains all the information of the process. Data such as the number of events, mass, energy and decay kinematics for all the particles involved are included. In addition, the time of flight for

both sneutrino and anti sneutrino for each event is also included. The mass of the sneutrino is set as 3.34×10^2 GeV, and the decay is specified to be into a muon and anti electron or anti muon and electron. The simulation was done for different input values of decay width. We finally opt for the decay width equal to 1.97×10^{-16} GeV to use it as reference to analyse the performance of the toy detector since produces a decay length inside the CMS detector (1 m).

The information in the LHE file is relevant at the parton level, for the "hard" part of the interaction. However, after this one needs to simulate "soft" QCD radiation. Moreover, physical particles include bound states. In order to simulate this we use Pythia8 [23]. Pythia8 is a tool based on C++ used for generating the "soft" part of the process in a high energy collision, it begins with the "hard" interactions and escalates to a multi particle complex final state. With all the information of the process generated, we are able to identify the trajectories and decays of the sneutrinos, and the same information for the products of their decays until they are at a final state. This way it is possible to analyze where the LLP decays and if it is detected or not. The procedure for this is the development of what we call a toy detector detailed in the following sub section.

4.2 The Toy Detector

The objective of this work was to design a toy detector of the CMS experiment based on Pythia8. This detector should be called from a main program that receives information of a process through an LHE file as an input and carries out the parton shower and hadronization. The toy detector itself receives as input a Pythia8 object per event, carrying the full information of the process, and returns the identification codes for the particles surviving cuts with information of where were they detected and their reconstructed momentum, taking into account the detector efficiency. For this, it executes a series of instructions per particle in the event detailed below. The toy detector and the main program were both based in [10].

Initially the particle passes through some general cuts. Each particle must be final, must not be a neutrino neither a neutral stable BSM particle. It must have a pseudorapidity not greater than 3 and its production length must be between the PV and the beginning of the MS, this because it is

the maximum length where a particle can be produced and yet be detected. If the particle passes all these constraints then it is possible for it to be detected therefore we start the analysis. In the case of studying a neutral LLP, the only possibility of being detected is by its decay products, therefore is important to know where these were produced.

We want to create a tag for each particle indicating in which sub detector it could be detected first. We start by defining two variables: the transverse production length (d_R) and the production length in the beam line (d_Z). For simplicity, we assume that the sub detectors all have a cylindrical shape. In Table 3 are specified all the considerations for the first stage assignment of these tags. We considered the four sub detectors (ID, ECal, HCal and MS) and also, for being able to determine where exactly was the particle produced, the superconducting solenoid. If d_R and d_Z are both equal to zero, the particle is prompt, we assign to it the tag "0". It is important to clarify that these are not exactly the dimensions of the sub detectors, these are the regions in which a particle can be produced and also detected in the same specific sub detector. As an example, consider a particle produced at $d_R = 0.6$ m and $d_Z = 1.0$ m, according to Table 1 is produced in the ID, but the ID is not capable of reconstructing the track, thus, the next sub detector that could be able to detect it is the ECal.

| Part of the Detector | Tag Assigned | d_{Rmax} [m] | d_{Zmin} [m] |
|--------------------------|--------------|----------------|----------------|
| ID | 1 | 0.500 | 2.900 |
| ECal | 2 | 1.770 | 3.540 |
| HCal | 3 | 2.950 | 5.549 |
| Superconducting Solenoid | 4 | 4.169 | 6.620 |
| MS | 5 | 5.000 | 8.000 |

Table 3: Initial considerations for the assignation of a tag that determines where a particle could first be detected. Data from [5]

Each sub detector cannot detect particles with pseudorapidity above a certain value. For instance, the ECal has a larger pseudorapidity coverage than the ID. We analyze the type of particle and pseudorapidity to determine in which sub detector the particle could indeed be detected. It is important to note that all the prompt charged particles with tag "0" would be first detected in the

ID, so the tag should be "1". The same situation arises with the particles produced in the superconducting solenoid, all of them would be detected in the MS, so the tag is changed from "4" to "5".

We previously restricted the pseudorapidity of all the incoming particles to $|\eta| < 3$, now we demand that the particles in the ID must have $|\eta| < 2.5$ and in the MS $|\eta| < 2.4$. If this constraint is not met in the ID, the tag changes from "1" to "2", and if it is not met in the MS, then the particle is not detected, and thus eliminated from the event.

Each sub detector is designed to recognize a specific type of particle depending on the structure and materials that compose it. The ID is able to detect only charged particles, then if a non charged particle is produced there, the tag changes from "1" to "2". The ECal only detects very light particles with electromagnetic interactions, namely electrons and photons, therefore if a particle is not one of them, the tag changes from "2" to "3". The HCal only detects hadrons, hence, if a particle is not a hadron then the tag switches from "3" to "5". Finally, the MS only detects charged particles, consequently if a non charged particle is produced in there, it is deleted from the event. If, at the end, a particle is considered detected, the information for identifying the particle and its respective sub detector tag is saved for later being used in the main program.

If the particle is detected we then "smear" the momentum. Smearing in particle physics refers to simulating the non perfect experimental reconstruction of the true value of momentum. To this end, we need the reported uncertainty of each sub detector (resolution). For each value of p_T we add to it the resolution of the sub detector multiplied by a random value of a Gaussian distribution with mean zero and standard deviation 1. The detected p_T has the form of:

$$p_{T\text{new}} = p_T \times (1 + \text{res} * \text{rndm Gauss})$$

where res is the resolution and rndm Gauss the random value of the Gaussian distribution.

The resolution function for each sub detector was obtained from Figures 2, 3 and 4. The ID and the HCal functions were obtained with a non linear fit, the function for the MS had a linear fit,

and the function of the ECal was given analytically. The ranges for p_T and $|\eta|$ are also specified on the graphs. For the ID and MS we obtained values of resolution for the pseudorapidity range not considered in Figure 2 by linear interpolation. All the fits were computed with Wolfram Mathematica. The computed p_{Tnew}/p_T for each sub detector are shown in Figures 12, 13, 14 and 15. We present a histogram that includes the combination of all sub detectors in Figure 16.

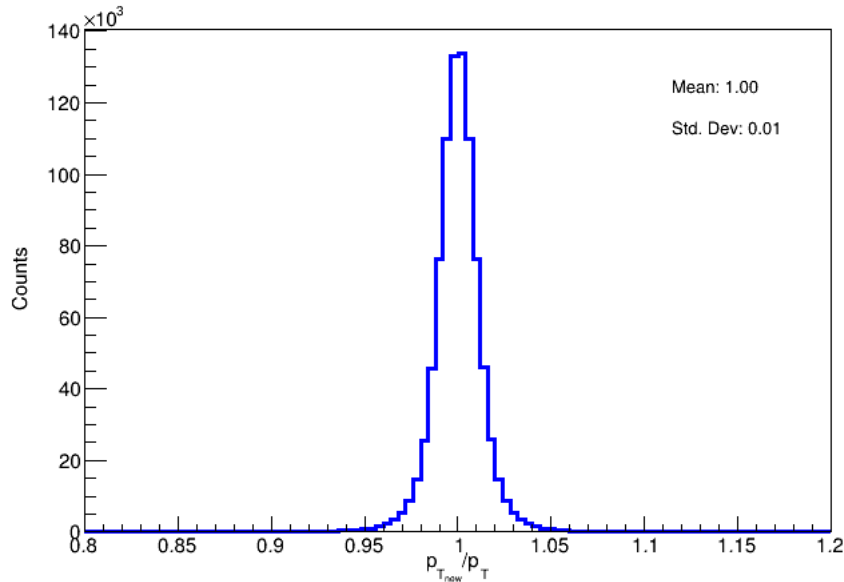


Figure 12: Histogram of p_{Tnew} / p_T in the ID.

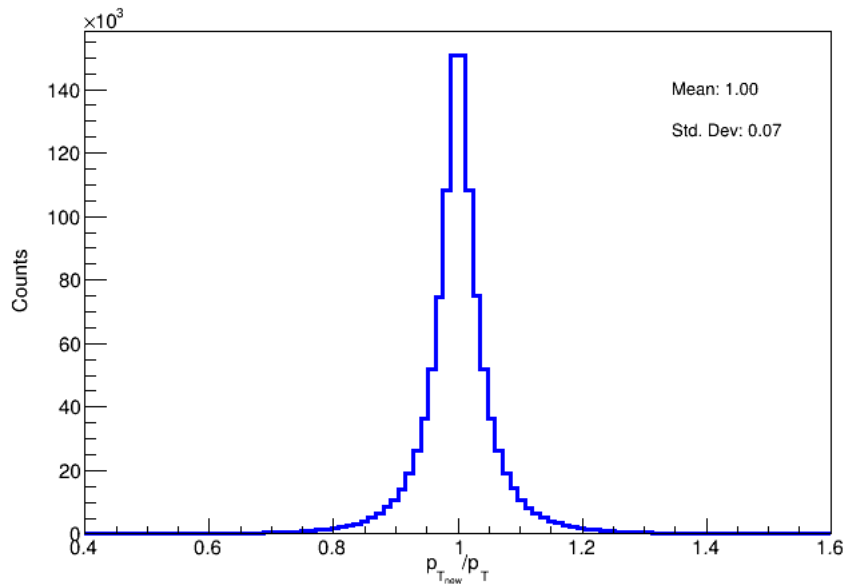


Figure 13: Histogram of $p_{T_{new}} / p_T$ in the ECal.

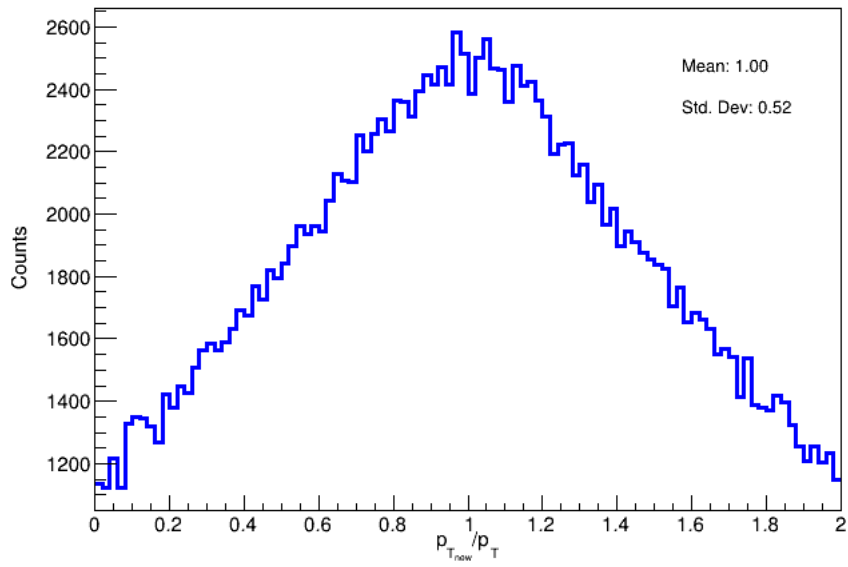


Figure 14: Histogram of $p_{T_{new}} / p_T$ in the HCal.

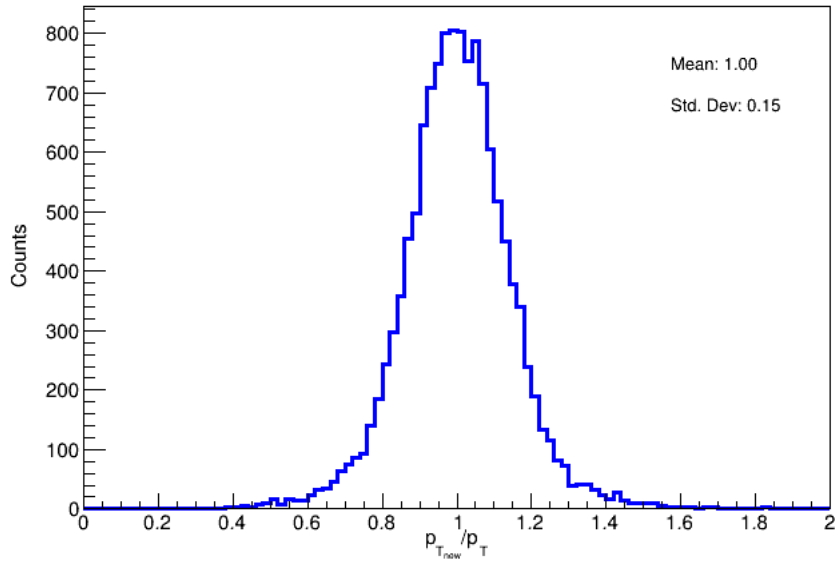


Figure 15: Histogram of $p_{T_{new}} / p_T$ in the MS.

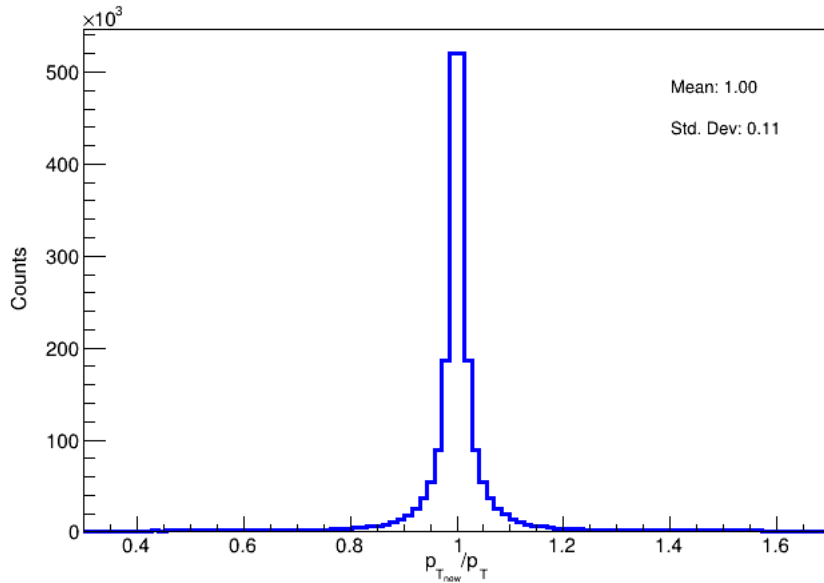


Figure 16: Histogram of $p_{T_{new}} / p_T$ in all the sub detectors.

In the near future we shall study LLPs decaying in the MS, leaving a shower of charged particles. In order to characterize this shower, we will need to know the average angular distance between each charged particle. Thus, as an exercise, we shall determine the minimum and maximum ΔR ,

where $\Delta R = \sqrt{(\Delta\eta)^2 + (\Delta\phi)^2}$, between one muon and any other charged particle in our generated events.

As mentioned before, this toy detector is run from a main program that calls the detector for each event generated and analyzes all the particles. From this program we compute ΔR . The program is receiving information of the detected particles mentioned before. Since the studied process generates an electron and a muon for each decay of LLP, the objective is to look for a ΔR that ideally includes both of them. This is why initially we chose to search for a muon in all the events.

We have to search for this muon in the information given by the toy detector to make sure it is detected. If it is, we then have information of its sub detector tag and smeared momentum. If the tag is "5", which means that it is located in the MS, then the muon is considered for the ΔR analysis. For this analysis two particles are needed, then another search is started. The only constraints for this new particle are: to be detected in the MS, to be charged, and not to have the same index of the muon already selected. When chosen the two particles, ΔR is calculated and, if it is less than all of the values calculated before in the same event, then it is the minimum ΔR and if it is bigger then it is the maximum ΔR . This was done for all the detected muons in the event. For each event we obtained a maximum and minimum value of ΔR and graph them as histograms (Figures 18 and 17). The minimum possible value for ΔR is zero and the maximum 5.57, this taking into consideration that the maximum $\Delta\eta$ in the MS is 4.6 and the maximum $\Delta\phi$ is π .

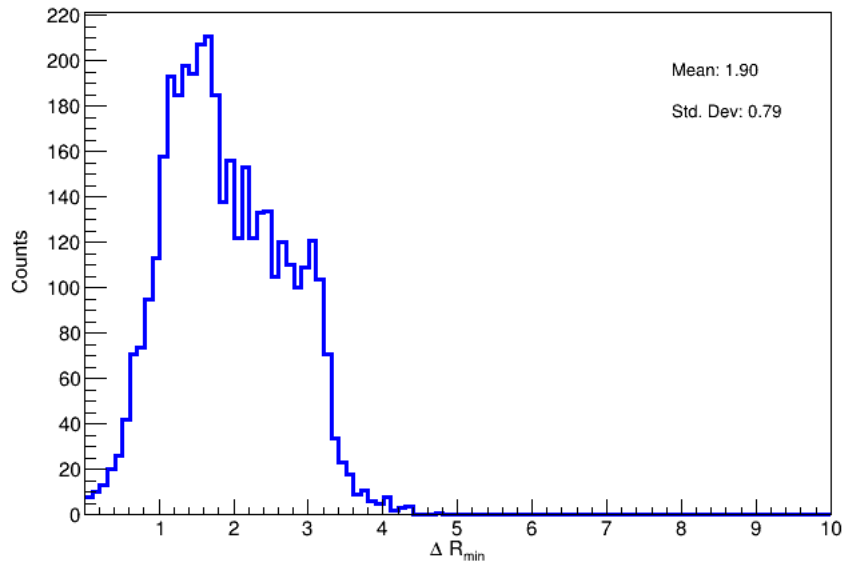


Figure 17: Histogram of ΔR_{min} .

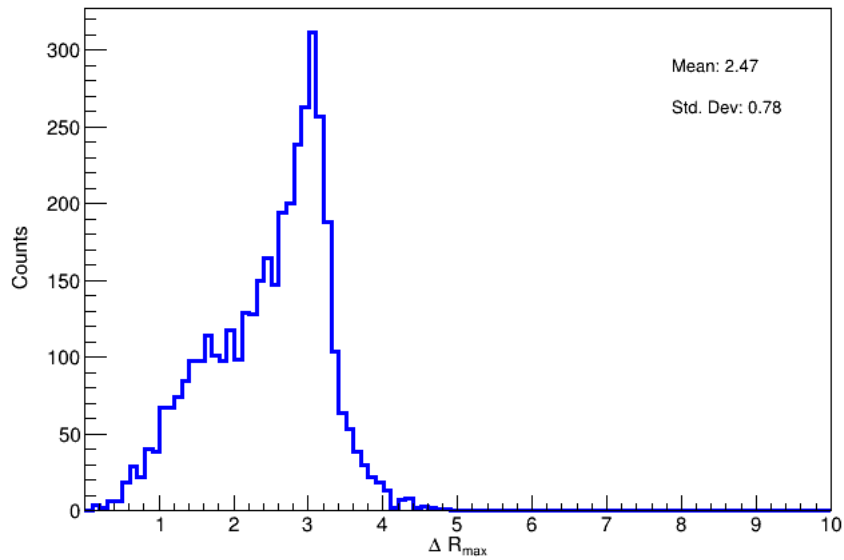


Figure 18: Histogram of ΔR_{max} .

5 Summary and Conclusions

In this work we presented a CMS toy detector based on C++ and Pythia8. The detector is capable of identifying if each of the particles in a simulated proton-proton collision event could be detected or not, considering factors such as dimensions of the sub detectors involved, pseudorapidity acceptance and type of particle being detected. This detector is also capable of identifying in what sub detector each particle could be initially identified. With this information, it analyses the energy or momentum resolution of the sub detector and returns a value for the smeared transverse momentum.

The objective of this toy detector is to create a tool for investigating a variety of models that involve neutral LLPs. For this reason, we presented a review of experimental searches and theoretical studies on LLPs, to be aware of what features the toy detector must have and to give an idea of the relevant cuts applied for this type of searches.

From the analysis and results presented in Section 4, we can conclude that the requested features of the toy detector have been appropriately implemented, such that a competitive search for a neutral LLP decaying between the IP and the beginning of the MS can be carried out soon.

References

- [1] M. Aaboud et al. “Search for long-lived particles in final states with displaced dimuon vertices in pp collisions at $\sqrt{s} = 13$ TeV with the ATLAS detector”. In: *Phys. Rev. D* 99 (1 Jan. 2019), p. 012001. DOI: 10.1103/PhysRevD.99.012001. URL: <https://link.aps.org/doi/10.1103/PhysRevD.99.012001>.
- [2] M. Aaboud et al. “Search for long-lived particles produced in pp collisions at $\sqrt{s} = 13$ TeV that decay into displaced hadronic jets in the ATLAS muon spectrometer”. In: *Phys. Rev. D* 99 (5 Mar. 2019), p. 052005. DOI: 10.1103/PhysRevD.99.052005. URL: <https://link.aps.org/doi/10.1103/PhysRevD.99.052005>.

- [3] Georges Aad et al. “Search for long-lived neutral particles decaying into lepton jets in proton-proton collisions at $\sqrt{s} = 8$ TeV with the ATLAS detector”. In: *JHEP* 11 (2014), p. 088. DOI: 10.1007/JHEP11(2014)088. arXiv: 1409.0746 [hep-ex].
- [4] V. M. Abazov et al. “Search for Neutral, Long-Lived Particles Decaying into Two Muons in $p\bar{p}$ Collisions at $\sqrt{s} = 1.96$ TeV”. In: *Phys. Rev. Lett.* 97 (16 Oct. 2006), p. 161802. DOI: 10.1103/PhysRevLett.97.161802. URL: <https://link.aps.org/doi/10.1103/PhysRevLett.97.161802>.
- [5] Elena Accomando et al. “Novel SM-like Higgs decay into displaced heavy neutrino pairs in $U(1)'$ models”. In: *JHEP* 04 (2017), p. 081. DOI: 10.1007/JHEP04(2017)081. arXiv: 1612.05977 [hep-ph].
- [6] Juliette Alimena et al. “Searching for Long-Lived Particles beyond the Standard Model at the Large Hadron Collider”. In: (Mar. 2019). arXiv: 1903.04497 [hep-ex].
- [7] J. Alwall et al. “The automated computation of tree-level and next-to-leading order differential cross sections, and their matching to parton shower simulations”. In: *JHEP* 07 (2014), p. 079. DOI: 10.1007/JHEP07(2014)079. arXiv: 1405.0301 [hep-ph].
- [8] Johan Alwall et al. “A Standard format for Les Houches event files”. In: *Comput. Phys. Commun.* 176 (2007), pp. 300–304. DOI: 10.1016/j.cpc.2006.11.010. arXiv: hep-ph/0609017.
- [9] Kyrylo Bondarenko et al. “Probing new physics with displaced vertices: muon tracker at CMS”. In: *Phys. Rev. D* 100.7 (2019), p. 075015. DOI: 10.1103/PhysRevD.100.075015. arXiv: 1903.11918 [hep-ph].
- [10] G. Brooijmans et al. “Les Houches 2017: Physics at TeV Colliders New Physics Working Group Report”. In: *10th Les Houches Workshop on Physics at TeV Colliders*. Mar. 2018. arXiv: 1803.10379 [hep-ph].

- [11] Matteo Cacciari, Gavin P. Salam, and Gregory Soyez. “FastJet User Manual”. In: *Eur. Phys. J. C* 72 (2012), p. 1896. DOI: 10.1140/epjc/s10052-012-1896-2. arXiv: 1111.6097 [hep-ph].
- [12] The CMS Experiment at CERN. *Detector*. URL: <https://cms.cern/detector>. (accessed: 27.07.2020).
- [13] The CMS Collaboration. “Search for long-lived neutral particles decaying to dijets”. In: (Oct. 2013).
- [14] The CMS Collaboration. “Search for long-lived particles that decay into final states containing two muons, reconstructed using only the CMS muon chambers”. In: (Apr. 2015).
- [15] The CMS Collaboration et al. “The CMS experiment at the CERN LHC”. In: *Journal of Instrumentation* 3.08 (Aug. 2008), S08004–S08004. DOI: 10.1088/1748-0221/3/08/s08004. URL: <https://doi.org/10.1088/1748-0221/3/08/s08004>.
- [16] Giovanna Cottin, Juan Carlos Helo, and Martin Hirsch. “Displaced vertices as probes of sterile neutrino mixing at the LHC”. In: *Phys. Rev. D* 98.3 (2018), p. 035012. DOI: 10.1103/PhysRevD.98.035012. arXiv: 1806.05191 [hep-ph].
- [17] Giovanna Cottin, Juan Carlos Helo, and Martin Hirsch. “Searches for light sterile neutrinos with multitrack displaced vertices”. In: *Phys. Rev. D* 97.5 (2018), p. 055025. DOI: 10.1103/PhysRevD.97.055025. arXiv: 1801.02734 [hep-ph].
- [18] Abhigyan Dasgupta. “Search for Long-Lived Particles Decaying to Displaced Dimuons at 13 TeV and Study of Neutron-Induced Background Hits in the Muon System of the Compact Muon Solenoid”. PhD thesis. UCLA, Los Angeles (main), 2019.
- [19] S. Dittmaier et al. “Handbook of LHC Higgs Cross Sections: 2. Differential Distributions”. In: (Jan. 2012). DOI: 10.5170/CERN-2012-002. arXiv: 1201.3084 [hep-ph].
- [20] Marco Drewes and Jan Hajer. “Heavy Neutrinos in displaced vertex searches at the LHC and HL-LHC”. In: *JHEP* 02 (2020), p. 070. DOI: 10.1007/JHEP02(2020)070. arXiv: 1903.06100 [hep-ph].

- [21] Vardan Khachatryan et al. “Search for long-lived particles that decay into final states containing two electrons or two muons in proton-proton collisions at $\sqrt{s} = 8$ TeV”. In: *Phys. Rev. D* 91.5 (2015), p. 052012. DOI: 10.1103/PhysRevD.91.052012. arXiv: 1411.6977 [hep-ex].
- [22] Matthew D. Schwartz. “TASI Lectures on Collider Physics”. In: *Proceedings, Theoretical Advanced Study Institute in Elementary Particle Physics : Anticipating the Next Discoveries in Particle Physics (TASI 2016): Boulder, CO, USA, June 6-July 1, 2016*. Ed. by Rouven Essig and Ian Low. 2018, pp. 65–100. DOI: 10.1142/9789813233348_0002. arXiv: 1709.04533 [hep-ph].
- [23] Torbjörn Sjöstrand et al. “An introduction to PYTHIA 8.2”. In: *Comput. Phys. Commun.* 191 (2015), pp. 159–177. DOI: 10.1016/j.cpc.2015.01.024. arXiv: 1410.3012 [hep-ph].
- [24] M. Tanabashi et al. “Review of Particle Physics”. In: *Phys. Rev. D* 98 (3 Aug. 2018), p. 030001. DOI: 10.1103/PhysRevD.98.030001. URL: <https://link.aps.org/doi/10.1103/PhysRevD.98.030001>.